Università degli Studi di Palermo

AREA RICERCA E TRASFERIMENTO TECNOLOGICO SETTORE
DOTTORATI E CONTRATTI PER LA RICERCA
U. O. DOTTORATI DI RICERCA

PhD Course in Biomedicine, Neuroscience and Advanced Diagnostics
Department of Biomedicine, Neuroscience and Advanced Diagnostics
SSD: MED/36

ROLE OF RADIOMICS IN PREDICTING BIOLOGICAL AGGRESSIVENESS AND PROGNOSIS OF PANCREATIC ADENOCARCINOMA

THE DOCTOR
MICHELA ANTONUCCI

THE COORDINATOR
PROF. FABIO BUCCHIERI

Firmato digitalmente da: Fabio Bucchieri Organizzazione: UNIVERSITA' DEGLI STUDI DI PALERMO/80023730825 Data: 18/06/2024 11:54:54

THE TUTOR
PROF. GIUSEPPE BRANCATELLI

XXXVI Cycle
Academic year 2020/2021

INDEX

Part 1 – Pancreatic Adenocarcinoma and Radiomics

1. INTRODUCTION

Pancreatic adenocarcinoma stands out as one of the most aggressive malignancies globally, characterized by its late diagnosis, limited treatment options, and dismal prognosis. Despite strides in imaging techniques and therapeutic modalities, overall survival rates for pancreatic cancer patients have seen scant improvement over recent decades. Consequently, there is a pressing need for innovative approaches to comprehensively comprehend the disease's heterogeneity, predict patient outcomes, and tailor personalized treatment strategies accordingly. In this context, recent breakthroughs in medical imaging and computational analysis have given rise to radiomics, an exciting field that extracts quantitative features from standard imaging modalities like computed tomography (CT) and magnetic resonance imaging (MRI). By scrutinizing a myriad of imaging characteristics, radiomics endeavors to scrutinize tumor attributes often imperceptible to the human eye, thus providing novel insights into tumor biology, prognosis, and treatment response.

1.1 Pancreatic adenocarcinoma

Pancreatic ductal adenocarcinoma (PDAC), constituting approximately 90% of all pancreatic cancer cases, is a profoundly malignant tumor (1). The prognosis for PDAC is predominantly based on the TNM-staging system (2). Despite extensive multidisciplinary efforts, the 5-year survival rate has shown only modest improvement, rising from 3.1% to 10% (1) (3).

The majority of these tumors, approximately 60-70%, are localized in the head of the pancreas, with the remaining 30-40% occurring in the body- tail region (4). The aggressive nature of pancreatic adenocarcinoma is well- documented: early diagnosis is achieved in only 7% of cases, while in 85% of cases, the disease is diagnosed at such an advanced stage that it is deemed unresectable. This underscores the significant challenges posed by pancreatic adenocarcinoma and highlights the urgent need for improved screening methods and treatment options (5).

1.1.1 Epidemiology and risk factors

Pancreatic adenocarcinoma is a significant global health concern, ranking as the sixth leading cause of cancer-related mortality worldwide. Its incidence is notably higher in industrialized countries, with rates of 28.7%/100,000 inhabitants in Europe and 13.1%/100,000 inhabitants in North America, compared to developing countries where the incidence is lower, at 3.7%/100,000 inhabitants in Africa (Figure 1).

Figure 1 – Incidence rates of pancreatic cancer globally (6).

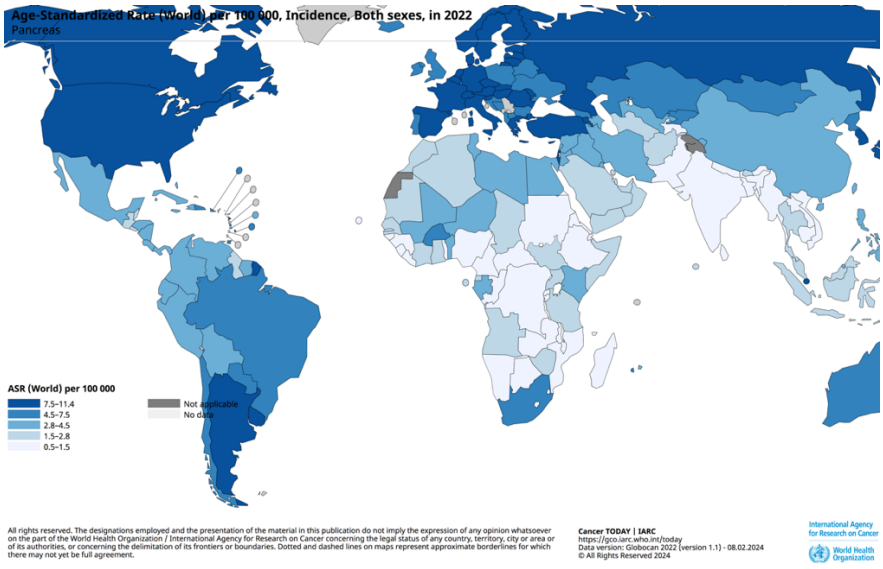

This disparity in incidence is largely attributed to environmental risk factors prevalent in industrialized nations (7). Furthermore, the incidence of pancreatic adenocarcinoma is steadily rising (8), with projections indicating that it may become the second most common cancer globally by the year 2030 (5).

This malignancy predominantly affects men more than women (9). Modifiable risk factors contributing to its development include cigarette smoking, which is estimated to confer a 25% increased risk, as well as obesity, sedentary lifestyle, and poor dietary habits. Studies (10) (11) (12) (13) have shown positive correlations between the consumption of red meat and animal fats and the risk of pancreatic cancer, while a negative correlation exists with the consumption of fruits, vegetables, and folates.

Non-modifiable risk factors include genetic mutations and predisposing familial syndromes, mucinous pancreatic cysts, diabetes mellitus, and chronic pancreatitis. Chronic infections such as hepatitis B virus (HBV), hepatitis C virus (HCV), and Helicobacter pylori (H. pylori) have been weakly associated with pancreatic adenocarcinoma, while the relationship with alcohol consumption remains inconclusive (14).

The intestinal microbiota appears to play a crucial role in the development of pancreatic adenocarcinoma, as disruptions in its composition can lead to chronic inflammation and the production of bacterial metabolites and toxins with carcinogenic properties (15).

Common genetic mutations observed in pancreatic adenocarcinoma include oncogenic mutations in genes like KRAS and loss-of-function mutations in tumor suppressors such as TP53, CDNK2A, DPC4/SMAD4, and BRCA2 (16). These genetic alterations contribute significantly to the pathogenesis of pancreatic adenocarcinoma and represent potential targets for therapeutic interventions.

1.1.2 Pathological anatomical features

The World Health Organization (WHO) classification delineates pancreatic cancer into benign, pre-malignant (referred to as PanIN), and malignant forms. Among the malignant forms, there are various histotypes, with ductal adenocarcinoma and its variants being the most prevalent (85-90%). Other histotypes include IPMN (Intraductal Papillary Mucinous Neoplasm) associated with invasive carcinoma (2- 3%), MCN (Mucinous Cystic Neoplasm) associated with invasive carcinoma (1%), solid pseudopapillary neoplasm (<1%), acinar cell carcinoma (<1%), and pancreatoblastoma (<1%) (17).

Pancreatic ductal adenocarcinoma (PDAC) represents the most commonly encountered pancreatic neoplasm. Macroscopically, on pathological examination, it presents as an isolated multinodular and sclerotic lesion with indistinct margins and a whitish cut surface. Histologically, PDACs are typically well-differentiated tumors surrounded by a prominent stromal reaction, which imparts a disorganized growth pattern and an obstructive character.

When mixed differentiation cells with a squamous component exceeding 30% are present in PDAC, it is classified as adenosquamous carcinoma (ASqC). This variant of PDCA, believed to be a metaplastic evolution, is more aggressive and less recognized, representing approximately 1-4% of exocrine malignant neoplasms.

Other rarely encountered variants include colloid carcinoma (non-cystic mucinous adenocarcinoma), hepatoid carcinoma characterized by areas reminiscent of pure liver carcinoma, medullary carcinoma (MCP) distinguished by a sparsely syncytial growth pattern accompanied by extensive intralesional necrosis, and undifferentiated carcinoma, predominantly located in the head of the pancreas, exhibiting varying consistencies from hard to rubbery, with occasional cystic and/or necrotic contents (18).

The differentiation of pancreatic carcinomatous lesions is one of the primary anatomopathological criteria for determining the resectability of pancreatic adenocarcinoma. This differentiation allows for the distinction between resectable tumors, borderline resectable tumors, locally advanced unresectable tumors, and metastatic tumors (19). The classification into these categories depends on factors such as the tumor's location within the pancreas, the degree of differentiation, and invasion of perineural, lymphatic, and vascular (arterial and venous) structures. Positivity to these parameters correlates with an unfavorable prognosis. Immunohistochemically, SMAD4 (55%) and overexpressed p53 are frequently detected.

1.1.3 Radiological diagnosis

When suspecting pancreatic neoplasia, the primary investigation methods employed are referred to as "cross-sectional imaging," namely CT and MRI with contrast medium (20). These imaging modalities play a pivotal role in diagnosing and screening pancreatic lesions.

CT currently serves as the gold standard for diagnosing pancreatic adenocarcinoma ≥2cm due to its widespread availability and repeatability. Although a single-phase CT scan at baseline may suffice for diagnosis, it is inadequate to evaluate tumor extension and distant metastases. A typical protocol involves biphasic CT with contrast medium, comprising two distinct phases:

- Parenchymal (or arterial) phase: facilitates lesion identification, size evaluation, extension assessment, and arterial vascular structure involvement (indicative of locally advanced disease). This phase is acquired 40-50 sec. after contrast medium bolus administration.
- Portal venous phase: optimizes visualization of the porto-mesenteric system, highlighting tumor involvement and revealing hepatic or peritoneal metastases or lymph node involvement. This phase is acquired 65-70 sec. post-contrast medium bolus administration (21).

The administration of contrast medium is imperative for receiving and characterizing pancreatic tumors. Contrast enhancement enables differentiation between tumor tissue and healthy tissue, facilitating evaluation of vascular invasion.

Pancreatic adenocarcinoma typically exhibits reduced vascularity, appearing hypodense on CT compared to surrounding parenchyma. It is often associated with pancreatic duct dilation (manifested by the "double duct" sign) and pancreatic atrophy downstream of the lesion. These secondary characteristics may aid in early diagnosis and screening of the neoplasm. However, in 10% of cases, patients may present with small, isodense, and contrast- enhancing lesions, complicating diagnosis. Dual-energy CT (DECT) utilizes different photon energy spectra to discriminate elements (calcium, iodine) in tissues that would otherwise exhibit similar attenuation on conventional CT. This allows for improved lesion detection and characterization, particularly for cystic masses, as well as therapeutic monitoring.

CT examination enables TNM staging of the neoplasm by evaluating its location, size (T), regional lymph node involvement (N), and the presence of vascular, perineural, and metastatic (M) involvement. Radiological documentation obtained from CT plays a pivotal role in determining staging and thus in defining a lesion as resectable or not.

Particular attention should be paid, in the report, to the presence of inflammatory outcomes at the parenchymal level, secondary to neoadjuvant chemotherapy, radiotherapy, or treatments like endoscopic retrograde cholangiopancreatography (ERCP) or echoendoscopy associated with biopsy. These may mimic viable tumor, complicating resectability assessment (20). CT sensitivity ranges from 76 to 96%, while MRI sensitivity ranges from 83 to 93.5% (20) (21) (23) (24).

MRI serves as a secondary examination and is performed in patients with CT scanning contraindications. It is also preferred for identifying small lesions that may be missed on CT. Pancreatic adenocarcinoma exhibits different appearances on MRI depending on the acquisition phase/sequence: hypointense on pre-contrast images; moderately hyperintense on T2. The diffusion-weighted sequence (DWI) enhances sensitivity for detecting lesions ≤3cm in diameter, aiding in differential diagnosis from mass-forming chronic pancreatitis. DWI detects water molecule diffusion restriction, secondary to histopathological alterations, allowing for improved lesion diagnosability, especially in patients with potentially resectable pancreatic adenocarcinoma (25).

Information obtained from diagnostic investigations allows for the evaluation of surgical resectability, particularly when aided by 3D imaging to study neoplastic mass relationships with surrounding vascular and parenchymal structures (26).

The 2020 AIOM Guidelines also recommend performing a biopsy examination with endoscopic ultrasound guidance in cases of "absence of clear signs of malignancy and patients not suitable for surgery," to obtain a definitive diagnosis (27) (28).

1.1.4 Therapeutic options

The treatment approach for pancreatic adenocarcinoma varies depending on the stage at which it is diagnosed: carcinoma detected at an early stage may be amenable to surgery aimed at complete resection, while carcinoma diagnosed at an advanced stage may necessitate palliative and symptomatic therapies aimed at maximizing the patient's quality of life (29). Surgical resection is the only treatment considered potentially curative. However, only a minority of patients (15-20% of total cases) are eligible for surgery due to diagnostic delays and vascular involvement at the time of diagnosis. The presence of liver, peritoneal, or other distant site metastases serves as an absolute contraindication to surgery. Partial involvement of arterial vessels (such as the superior mesenteric artery, aorta, or celiac tripod) and venous vessels (such as superior mesenteric vein, portal vessels, or inferior vena cava) constitutes a relative contraindication, often necessitating neoadjuvant therapy (radiotherapy and/or chemotherapy) before determining surgical suitability. Different types of surgery may be performed based on the location (head, body, and/or tail of the gland) and the extent of the mass, including pancreaticoduodenectomy or pancreatectomy, either complete or distal, sometimes combined with splenectomy. Additionally, more or less extensive lymphadenectomy may be required (30). Current pharmacological protocols for neoadjuvant and post-operative therapy include FOLFOX (comprising 5-fluorouracil, leucovorin and oxaliplatin), FOLFIRINOX (comprising 5-fluorouracil, leucovorin, irinotecan, and oxaliplatin), and Gemcitabine. Meanwhile, ongoing research endeavors are focused on discovering new biological drugs that can facilitate increasingly targeted and functional therapy approaches (27) (31) (32).

1.1.1 Prognosis

Prognosis in pancreatic adenocarcinoma varies depending on the histological grade and stage of the neoplasm, but most significantly, on the treatment approach adopted. Generally, prognosis is more favourable for patients who undergo surgical treatment with complete resection of the tumor, although the majority of these individuals still succumb to disease-related complications. Patients who do not undergo surgical treatment may experience slightly differing prognoses based on the stage, but outcomes typically remain poor regardless (33).

1.2 RADIOMICS

Radiomics represents a cutting-edge frontier in medicine, aiming to extract quantitative information from radiological images. By harnessing advanced computational techniques, radiomics facilitates the extraction of a vast array of quantitative features from medical images, transcending traditional visual interpretation. This approach enables the characterization of tissue heterogeneity, spatial distribution of imaging biomarkers, and subtle patterns that may not be discernible to the naked eye. Radiomics holds immense promise in revolutionizing disease diagnosis, prognosis, and treatment response assessment across various medical disciplines, offering a deeper understanding of disease biology and personalized patient care.

1.2.1 Basic principles

The digitization of radiological sciences has transformed simple images into intricate arrays of pixels, which, when rendered in grayscale, offer insights into the diverse textures of tissues. Radiomics aims to enhance image evaluation by extrapolating a vast amount of data from the shape and heterogeneity of a lesion, providing pathophysiological insights that may not be discernible to the naked eye. These data, when combined with genomic, proteomic, transcriptomic, and other datasets, offer comprehensive and intricate information beyond what can be

derived from simple visual observation. This expanded information spectrum enables diagnosis, prognostic predictions, and monitoring of lesion evolution during follow-up, both pre- and post-application of radiopharmacological treatments. Traditionally, tumor heterogeneity, considered a prognostic determinant of survival, has been studied through pathological anatomy, analyzing fragments or portions of a tumor mass. However, with radiomics, tumor heterogeneity can now be studied across the entire volume of the lesion. While radiomics initially focused on oncological lesions, particularly focal ones, its scope is expanding to encompass non-oncological and widespread pathologies (34) (35).

Radiomics analysis entails several phases (figure 2):

1. image acquisition and segmentation;
2. features extraction and qualification;
3. data handling and analysis;
4. model building.

.

Figure 2 – The workflow of radiomics analysis (36).

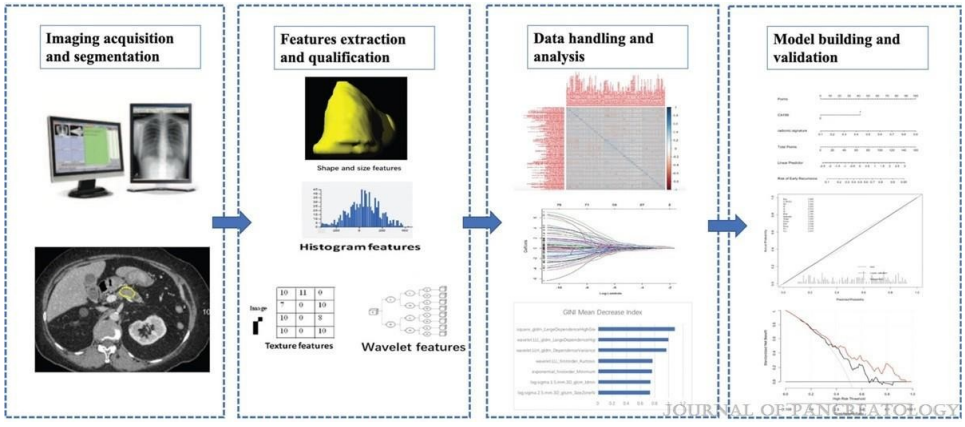

Among these phases, segmentation is critical. While automated segmentation using advanced software is possible, manual segmentation is often preferred for its precision, albeit being operator- dependent. Artificial intelligence may be susceptible to imaging artifacts, which could distort the selection of regions of interest, thus compromising results.

Another crucial stage is the extraction and characterization of features, also known as "high-dimensional features" or more commonly, "big data," owing to the multitude of variables identified. Once extracted, this data is used to develop classification models for predicting outcomes.

Ultimately, the goal of radiomics is to enhance non-invasive diagnostic investigation methods by correlating imaging techniques with molecular and pathological analyses of lesions.

1.2.2 Texture features

The quantitative data extracted from radiological images are derived from texture evaluation through textural analysis. Textural analysis delves into the characteristics of lesions in terms of intensity heterogeneity, which is detectable in single or correlated pixels and contextualized within specific regions of interest obtained through segmentation.

While an in-depth understanding of radiomics features is not essential, it can aid in comprehending the results. Among the features are statistical ones (based on histograms and textures), model-based features, transformation-based features, and shape-based features. These features can be extracted from both two-dimensional and three-dimensional regions of interest.

Texture features primarily rely on the diverse gray intensities between adjacent pixels/voxels and the arrangement of various gray shades in multidimensional matrices. Key texture features include:

- Absolute gradient: Measures the degree of gray variation between adjacent pixels/voxels, with maximum variation in black-white comparison and minimum in white-white or black-black comparison.

- Gray-level Co-occurrence Matrix (GLCM): Defines the spatial relationship between pairs of pixels/voxels in different directions.

- Gray-Level Run-Length Matrix (GLRLM): Provides information on the spatial distribution of consecutive pixels with the same gray level in

multiple directions.

- Gray-Level Size Zone Matrix (GLSZM) and Gray-Level Distance Zone Matrix (GLDZM): Characterizes groups or zones of pixels/voxels with the same gray levels.

- Neighborhood Gray-Tone Difference Matrix (NGTDM): Quantifies the difference between the gray levels of a pixel or voxel and the primary gray level of neighboring pixels or voxels within a predefined distance.

- Neighborhood Gray-Level Dependence Matrix (NGLDM): Establishes the connection between a pixel/voxel and its neighborhood based on the range differences in gray levels (35).

1.2.3 Segmentation techniques

Segmentation involves identifying and delineating the area of the lesion being studied in two or three dimensions, thereby defining the regions of interest and volumes of interest, respectively.

Various techniques can be employed for segmentation:

- Manual segmentation involves the manual delineation of the lesion's boundary by an operator.

- Semi-automatic segmentation utilizes standard image segmentation algorithms to identify the lesion's growth region or perimeter, followed by manual refinement if necessary.

- Automatic segmentation relies on deep-learning algorithms, a type of machine learning based on multi-level models (37). This technique allows for rapid segmentation of a large number of lesions without significant intra- or inter-observer variability.

Manual and semi-automatic techniques are commonly used and are sometimes more precise than automatic methods. However, they require more time for lesion selection and are operator-dependent. In contrast, automatic segmentation techniques offer rapid processing but may lose reliability in the presence of artifacts that could confuse the software (38).

1.2.4 Applications in the pancreas

Over time, radiomics has emerged as a promising method for studying both focal and diffuse lesions of the pancreas (39). Numerous studies have underscored the potential of radiomics applied to this organ, with a focus on various aspects such as differential diagnosis between malignant and benign lesions, as well as between malignant lesions of different types. To date, research has identified differences between pancreatic ductal adenocarcinoma lesions and healthy tissue (40), focal pancreatitis (41), neuroendocrine tumors (42), pancreatic lymphoma (43), and autoimmune pancreatitis (44). Additionally, studies have explored the prediction of survival in patients with pancreatic ductal adenocarcinoma who undergo initial surgical resection (45).

Despite these advancements, the use of radiomics has not yet been validated for differentiating the histological grade of pancreatic ductal adenocarcinoma. This represents an area of ongoing research and exploration within the field of radiomics.

Part 2 – Original Research: Role of radiomics in predicting biological aggressiveness and prognosis of pancreatic adenocarcinoma

2 THE STUDY

2.1 PURPOSE

This study aims to investigate the efficacy of radiomics analysis using contrast-enhanced CT images in distinguishing between different histological grades of pancreatic ductal adenocarcinoma. The ultimate goal is to offer reliable and non-invasive assistance by establishing a correlation between radiomic features and histopathological data. Such correlations could significantly enhance the clinical decision-making process, aiding in the prediction of biological aggressiveness and prognosis of pancreatic adenocarcinoma.

2.2 MATERIALS AND METHODS

Our retrospective study, initiated in 2020, stemmed from a collaborative effort between the "Paolo Giaccone" University Hospital and the "La Maddalena" Level III Oncology Department. This multicenter collaboration aimed to pool resources and expertise in order to conduct a comprehensive analysis on pancreatic adenocarcinoma.

2.2.1 POPULATION

For this study, 155 patients with pancreatic lesions were recruited, selected based on specific inclusion criteria:

- Age >18 years.
- Diagnosis of pancreatic lesion subjected to resection.
- Patients undergoing CT and MRI investigations with contrast medium, including examination of the parenchymal and portal phases.
- Patients not undergoing pre-resection treatment.

Patients were excluded based on the following criteria (Figure 3):

- Presence of secondary or primary lesions other than adenocarcinoma.
- Patients who did not undergo CT/MRI examination or did not undergo evaluation with contrast medium.

The initial population consisted of 155 patients, comprising n=81 women (51.9%) and n=74 men (48.1%), aged between 44 and 90 years, who underwent resection surgery of the pancreatic lesion between 2009 and 2020. Among these patients, n=104 underwent CT, including n=5 who had baseline CT, while n=55 underwent MRI, with n=3 undergoing baseline MRI.

The resected pancreatic lesions included:

- Pancreatic ductal adenocarcinomas (n=90)

- Papilla neoplasms (n=12)
- Neuroendocrine carcinomas (n=10)
- Duodenal neoplasms (n=6)
- Metastatic lesions of primary non-pancreatic tumors (n=5)
- Cholangiocarcinomas (n=4)
- Unspecified lesions (n=3)
- Serous cystadenocarcinomas (n=2)
- Inflammation (n=2)
- GIST (Gastrointestinal Stromal Tumors) (n=2)
- Lymphomas (n=2)
- Mucinous cystic neoplasms (n=2)
- Pseudopapillary solid epithelial neoplasms (n=2)
- Gastric neoplasms (n=2)
- Adrenal neoplasms (n=2)
- Cysts (n=1)
- Solitary cysts (n=1)
- Dysplastic lesions (n=1)
- Intestinal neoplasms (n=1)

- Hyperplastic lesions (n=1)
- IPMN (Intraductal Papillary Mucinous Neoplasm) (n=1)
- Mucinous neoplasms (n=1)
- Chronic pancreatitis (n=1)
- Squamous neoplasms (n=1).

Figure 3 – Flow diagram of the study population

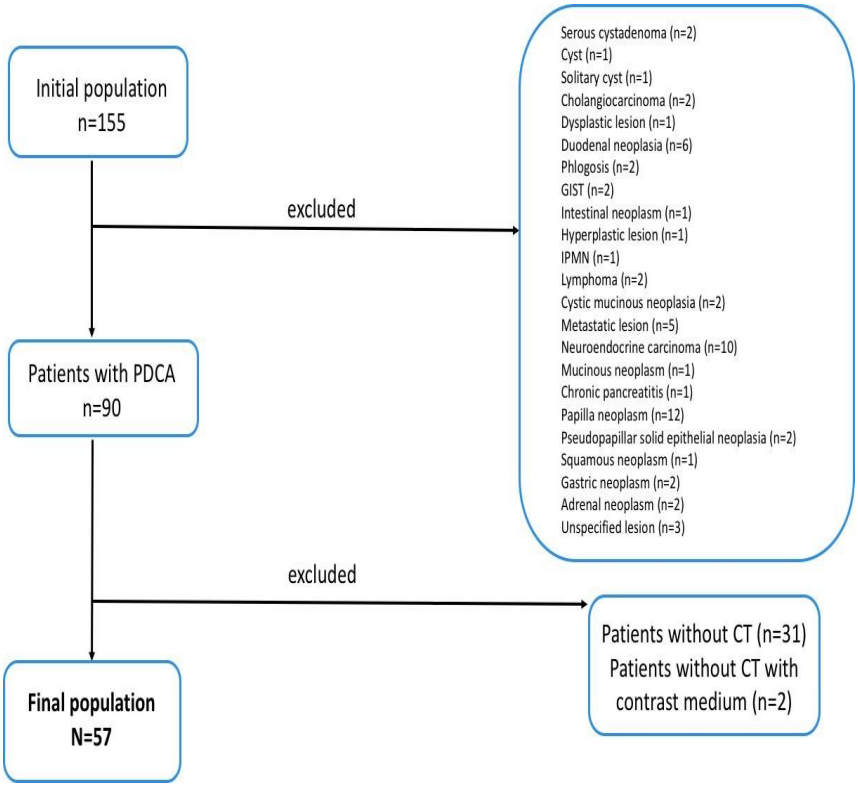

2.2.2 IMAGING TECHNIQUE – CT PROTOCOL

Multiphasic CT investigations were conducted using a 128-detector row CT scanner. Each investigation followed a study protocol designed to examine the pancreatic parenchyma. This protocol included an initial acquisition before the administration of contrast medium, followed by a pancreatic phase at 35-40 seconds, acquired using the bolus tracking technique. Subsequently, a venous phase was captured 65-70 seconds after the administration of the contrast medium.

The post-contrast study involved the intravenous administration of 110-
120 ml of non-ionic contrast medium, such as 400 mg/ml Iomeprol (Iomeron 400, Bracco Imaging, Milan, Italy), 370 mg/dl Iopromide (Ultravist 370, Bayer Pharma), or 350 mg/dl Iobitidrol (Xenetix 350, Guerbet; Omnipaque 350, GE Healthcare AS), depending on availability or at the discretion of the radiologist. The contrast medium bolus was administered through a venous catheter (18-20 gauge) using an injector at a flow rate of 3-5 mL/s, followed by a 20 mL saline bolus at the same flow rate.

2.2.3 SEGMENTATION AND EXTRACTION

Initially, manual segmentation was performed by two radiologists, one of whom expert, blinded. Each contrast-enhanced CT exam was anonymized, imported into an open-source DICOM viewer, and sent in DICOM format to a dedicated workstation integrated with radiomics analysis software called ITK-SNAP (Figure 4 and 5). Regions of interest were delineated in all slices where the lesion was visible in both the pancreatic and portal phases, resulting in a three-dimensional segmentation of the lesion (Figure 6, 7 and 8). A computer engineer was tasked with extracting data from the texture analysis using PyRadiomics (Figure 9) -version 3.0- software (46). For each region of interest, 120 radiomic parameters were obtained, including first-order parameters (which provide information related to the gray level distribution without considering spatial relationships between voxels), second-order parameters (which consider spatial relationships between voxels), and third-order parameters (which consider relationships between a number of voxels ≥3). The texture parameters were calculated from histogram analysis of gray levels (e.g., mean, variance, skewness, kurtosis, and percentiles). Additionally, the co-occurrence matrix was calculated using five measurements (e.g., contrast, correlation, sum of squares, inverse difference moment, sum average, sum variance, sum entropy, difference variance, difference entropy), while the run-length matrix was calculated in four directions (e.g., run length non uniformity, grey-level non uniformity normalized, long run emphasis, short run emphasis). Later, we investigated the segmentation and resulting radiomic feature variations due to the inter-observer variability, involving two other radiologists, of which another expert.

Figure 4 and 5 – ITK-SNAP software application: Allows you to segment MRI and CT scan images, viewed in 3 planes of space, for clinical and research purposes.

Figure 6 – Example of segmentation in a 70-year-old patient with pancreatic adenocarcinoma at the level of the pancreatic body (arrow). Segmentation was performed in the pancreatic phase (A and B) and in the portal phase (C and D).

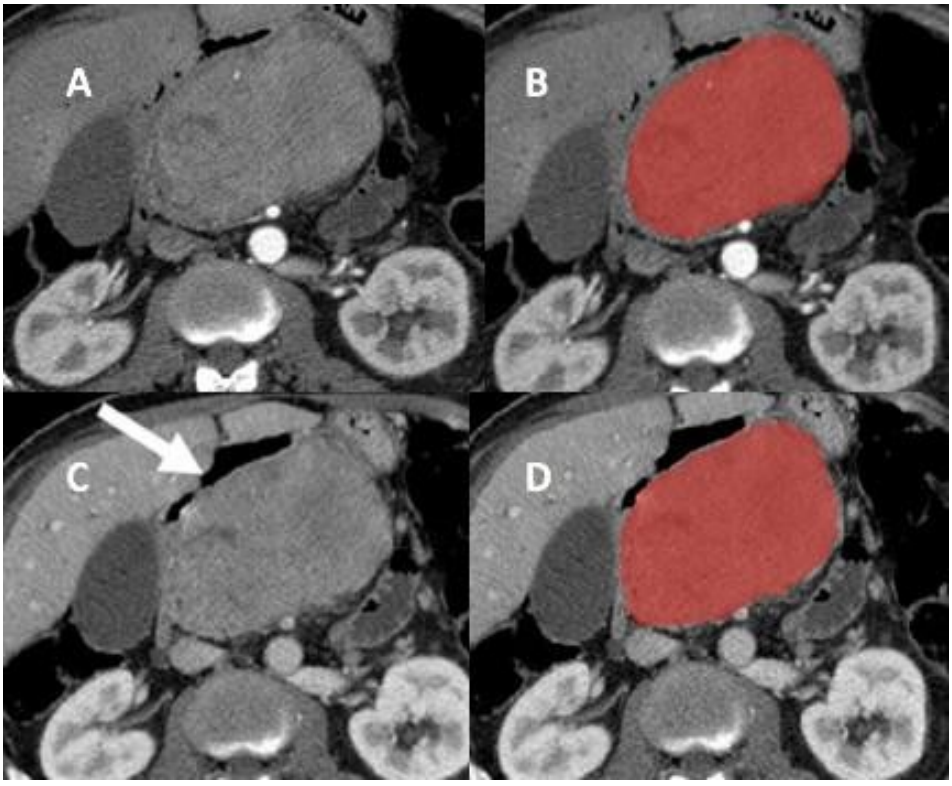

Figure 7 – Example of segmentation in a 67-year-old patient with pancreatic adenocarcinoma at the level of the pancreatic body (arrow). Segmentation was performed in the pancreatic phase (A and B) and in the portal phase (C and D).

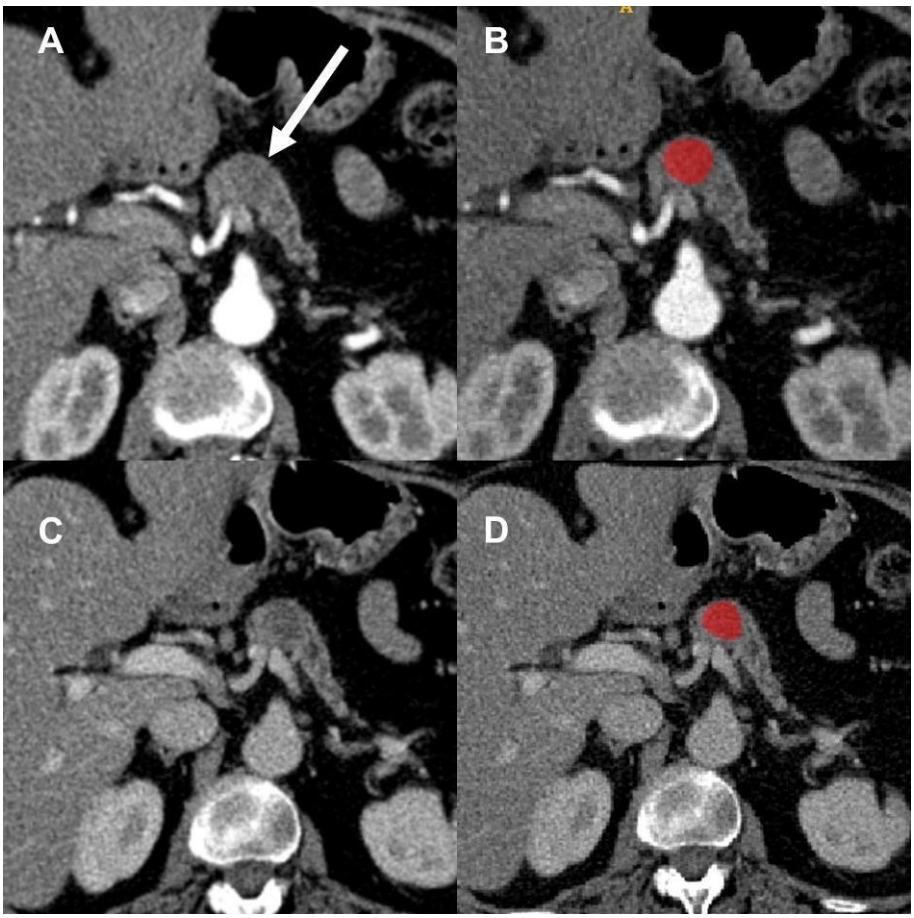

Figure 8 – Example of segmentation in a 55-year-old patient with pancreatic adenocarcinoma at the level of the pancreatic head (with arrow) with presence of biliary stent (yellow arrow). Segmentation was performed in the pancreatic phase (A and B) and in the portal phase (C and D).

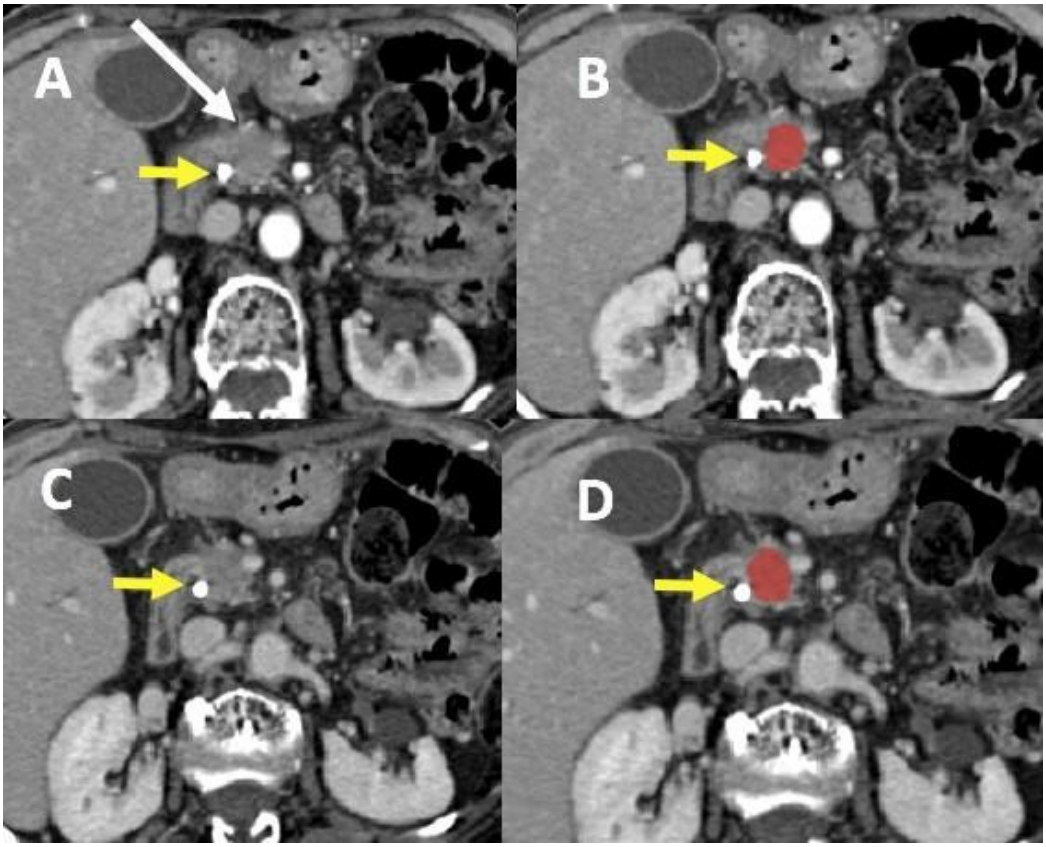

Figure 9 – Overview figure of the process of PyRadiomics. First, medical images are segmented. Second, features are extracted using the PyRadiomics platform, and third, features are analyzed for associations with clinical or biologic factors.

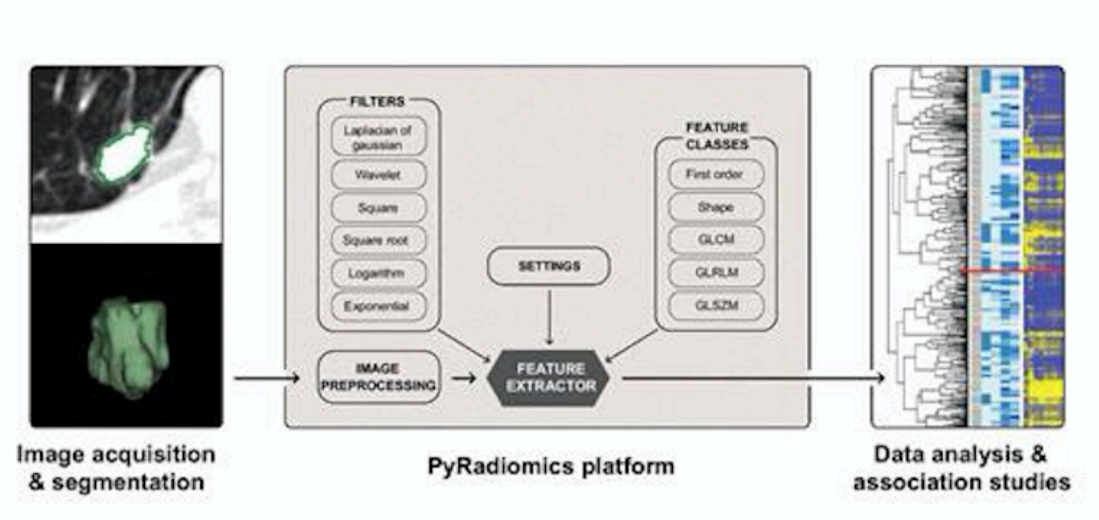

2.2.4 REFERENCE STANDARDS

Anatomopathological confirmation, obtained post-surgical resection of the lesions, served as the gold standard for diagnosis. During histological fragment resection, the surgeon marked the margins to ensure proper orientation and precise perpendicular cutting of the tumor.

A specialized anatomopathologist, focusing on pancreatic pathology, assessed various histological parameters including histological grading, margins, vascular invasion, perineural invasion, and metastatic lymph nodes.

Histological grading denotes the level of cellular differentiation of a tumor relative to its tissue of origin, reflecting the proportion of undifferentiated cells. This grading is closely associated with tumor aggressiveness: a mass primarily comprising well-differentiated cells suggests lower aggressiveness, with slower growth rates and a lower likelihood of metastasis. Conversely, a mass predominantly composed of undifferentiated cells indicates higher aggressiveness, capable of migrating through blood, lymphatic, or perineural routes, leading to distant metastases.

Different grades are distinguished (47):

- Gx: Indeterminate grade;
- G1: Well-differentiated (<25% undifferentiated cells);
- G2: Moderately differentiated (<50% undifferentiated cells);

- G3: Poorly differentiated (50-75% undifferentiated cells);
- G4: Undifferentiated (>75% undifferentiated cells).

Assessing margins for tumor cell presence is crucial; cells at the margin indicate residual disease, signifying incomplete tumor resection (48) (49) (50). Different degrees of residual disease are classified based on tumor cell presence (51):

- R0: Absence of tumor cells;
- R1: Microscopic tumor residues;
- R2: Macroscopic tumor residues.

Invasion of neuronal, vascular, and lymphatic structures indicates tumor progression beyond the pancreas. Vascular invasion, affecting arterial and venous structures, occurs when tumor cells breach vessel walls and enter circulation.

Perineural invasion, occurring when tumors invade nerve structures, signifies heightened aggressiveness. Pancreatic adenocarcinoma particularly exploits the nearby rich neural network near the uncinate process, involving the celiac plexus and associated ganglia (52).

Lymph node involvement is another unfavorable prognostic factor. Lymph nodes adjacent to the tumor are removed during resection for histopathological examination. Positive findings suggest tumor spread through lymphatic pathways, increasing the risk of lymph node metastasis (53).

2.2.5 STATISTIC ANALYSIS

The statistical and computational analysis was conducted by the same engineer responsible for extracting data from the regions of interest. For each phase (parenchymal and portal), various outcomes including differentiation, perineural invasion, vascular invasion, metastatic lymph nodes, and margins were assessed. To identify the most discriminative features, the punctual biserial correlation index was calculated between continuous variables and the dichotomous variable (reference standard), assuming values of 1 or 0.

Discriminant analysis was employed to assess the performance of the radiomics model. Eighty percent of the samples were allocated for training the classifier, while the remaining 20% were reserved for testing its classification reliability. Predictive assessment of sensitivity, specificity, and accuracy was conducted for each selected outcome. Furthermore, p-values were computed, ROC curves were generated, and the areas under the curve (AUROC) along with their 95% confidence intervals were evaluated to gauge the diagnostic performance of the studied outcomes.

The computational statistical analysis proposed was implemented using the MatLab R2019a simulation environment (MathWorks, Natick, MA, USA). Radiomic features from both the arterial and portal phases were subjected to robustness analysis using the intraclass correlation coefficient (ICC). ICC was calculated considering all four observers and separately for expert and non-expert observers.

The ICC estimates were categorized to indicate poor (ICC < 0.30), moderate (0.30 < ICC < 0.60), good (0.60 < ICC < 0.80), and excellent reliability (ICC > 0.80) of radiomic characteristics compared to reference results.

Additionally, ICC was utilized to determine the reproducibility of radiomics features based on tumor location, pathological diameter, and the presence of biliary stents.

2.3 RESULTS

2.3.1 POPULATION

As depicted in Table 1, out of the initial population of 155 patients, a subset of 57 individuals was selected, with an average age of 73.5 years. Among these, there were 26 (45.6%) males and 31 (54.4%) females, all diagnosed with pancreatic ductal adenocarcinoma and evaluated through contrast-enhanced CT in both arterial and portal phases.

Regarding the isolated lesions, which had an average diameter of 3.7cm, 43 (75.4%) were classified with G1-G2 grading, while 14 (24.6%) were classified with G3 grading. Margin involvement was observed in 29 cases (50.9%), whereas 28 cases (49.1%) had clear margins. Vascular invasion was present in 16 cases (28.1%) and absent in 41 cases (71.9%). Perineural invasion was found in 44 cases (77.2%), while 13 cases (22.8%) showed no perineural invasion. Lymph node metastases were detected in 40 patients (70.2%), while 17 patients (29.8%) did not exhibit lymph node involvement. Distant metastases, indicating non-resectable criteria, were identified post-resection in only 5 cases (8.8%).

Table 1 – Characteristics of the study population

Variables	
Sex-n. (%) -Males -Females	26 (45,6%) 31 (54,4%)
Mean age (years)	73,5
Mean lesion diameter (cm)	3,7
Grading -G1-G2 -G3	43 (75,4%) 14 (24,6%)
Margins-n. (%) -Involved -Indemnified	29 (50,9%) 28 (49,1%)
Vascular invasion-n. (%) -Present -Absent	16 (28,1%) 41 (71,9%)
Perineural invasion-n. (%) -Present -Absent	44 (77,2%) 13 (22,8%)
Lymph node metastases-n. (%) -Present -Absent	40 (70,2%) 17 (29,8%)
Distant metastases -n. (%) -Present -Absent	5 (8,8%) 52 (91,2%)

2.3.2 RADIOMIC ANALYSIS

As illustrated in Table 2, among the observed features, the radiomics feature "original NGTDM contrast" emerged as the most statistically significant predictor for the "differentiation" outcome, evident in both the arterial and portal phases, with a p-value of <0.001 in both instances. This suggests a strong association between this specific radiomics feature and the differentiation status of the lesions, highlighting its potential as a valuable diagnostic marker in both phases of contrast-enhanced CT imaging.

Table 2 – Characteristics identified by the statistical system based on the point-biserial correlation coefficient.

OUTCOME	ARTERIAL PHASE		PORTAL PHASE	
	Feature	**P-value**	**Feature**	**P-value**
Differentiation	Original NGTDM contrast	<0,001	Original NGTDM contrast	<0,001
Perineural invasion	Original GLSZM Size Zone Non Uniformity	0,052	Original GLSZM Large Area High Gray-Level Emphasis	0,057
	Original First Order Interquartile Range	0,023		
Vascular invasion	Original First Order Maximum	0,181	Original NGTDM contrast	0,051
	Original Shape Maximum 2D Diameter Slice	0,050		
Lymph node metastases	Diagnostics Image original Minimum	0,014	Diagnostics Image original Minimum	0,014
	Original Shape Maximum 2D Diameter Slice	0,001		
Margins	Original GLSZM Low Gray-Level Zone Emphasis	0,050	Original GLCM Autocorrelation	0,032

The results encompassing sensitivity, specificity, accuracy - expressed as percentages -, AUROC with 95% confidence interval, and corresponding p-values for each outcome are detailed in Table 3.

In the arterial phase, differentiation emerges as the outcome with the highest statistical significance ($p<0.001$). It demonstrates a sensitivity of 67.1%, specificity of 86.2%, accuracy of 72%, and an AUROC value (95% CI) of 0.762 (0.597-0.927) for predicting poorly differentiated lesions (G3).

Similarly, in the portal phase, differentiation stands out as the outcome with the most robust statistical performance ($p=0.004$). It exhibits a sensitivity of 76.0%, specificity of 60.9%, accuracy of 71.9%, and an AUROC value (95% CI) of 0.758 (0.600-0.916) for predicting poorly differentiated lesions (G3). The ROC curves of the most discriminating feature in the arterial (A) and portal (B) phase for predicting outcomes with better statistical performance are depicted in Figures 9, 10, 11, 12 and 13.

Table 3 – Performance of the discriminant analysis models based on the selected features.

Outcome	Sensitivity	Specificity	Accuracy	AUROC (95% CI)	P-value
ARTERIAL PHASE					
Differentiation	67.1%	86.2%	72%	0.762 (59,7%-92,7%)	<0.001
Perineural invasion	37.6%	83.7%	73.7%	0.680 (48,1%-87,9%)	0.294
Vascular invasion	57.8%	48.3%	55.1%	0.630 (46,9%-79,1%)	0.616
Lymph node metastases	69.7%	83.4%	79.4%	0.739 (58,6%-89,2%)	0.510
Margins	57.03%	49.0%	53.0%	0.601 (44,7%-75,4%)	0.194
PORTAL PHASE					
Differentiation	76.0%	60.9%	71.9%	0.758 (60,0%-91,6%)	0.004
Perineural invasion	5.9%	98.0%	79.9%	0.467 (24,4%-69,0%)	0.792
Vascular invasion	55.5%	60.1%	59.0%	0.638 (47,5%-80,0%)	0.082
Lymph node metastases	53.5%	83.0%	74.4%	0.618 (43,6%-80,0%)	0.212
Margins	63.2%	54.8%	58.9%	0.637 (48,7%-78,6%)	0.088

Figure 9 – ROC curve of the most discriminating feature on the arterial **(A)** and portal **(B)** phases for the prediction of poorly Differentiated lesions (G3).

(A)

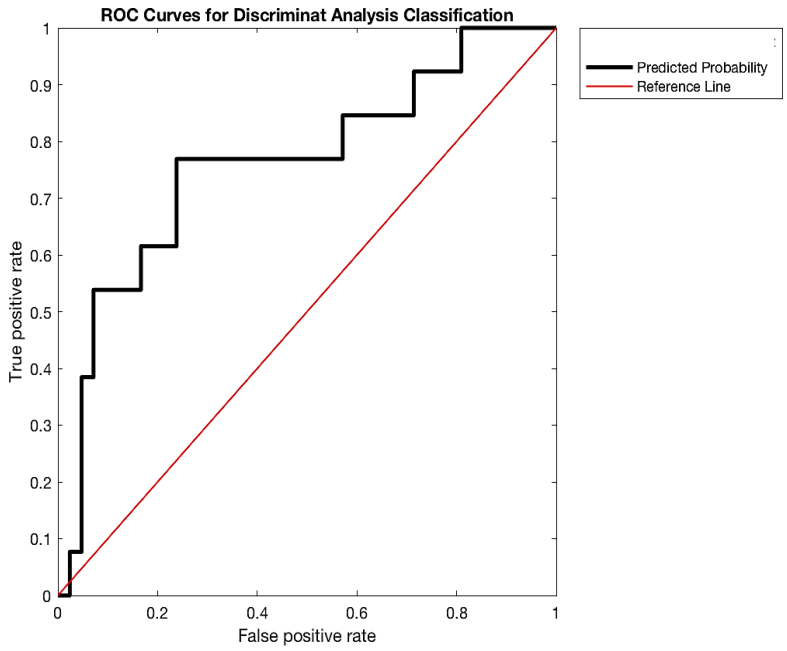

(B)

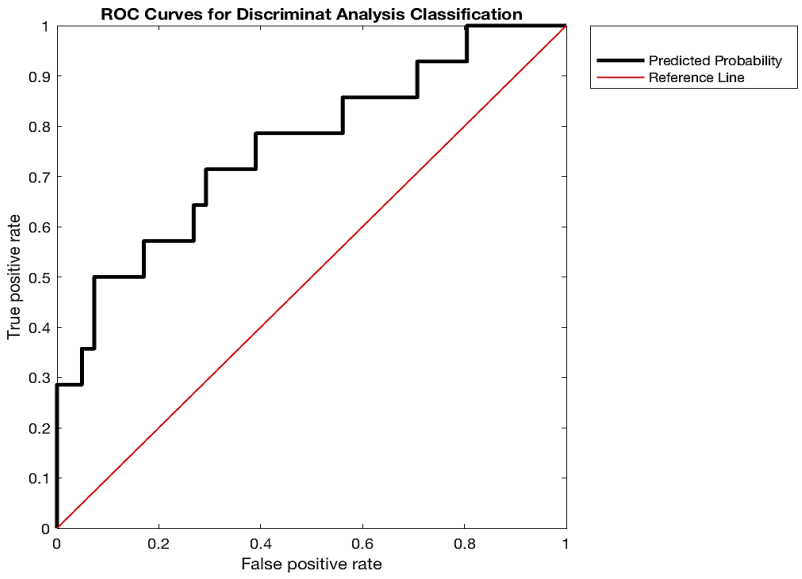

Figure 10 – ROC curve of the most discriminating feature on the arterial **(A)** and portal **(B)** phases for the prediction of Perineural invasion.

(A)

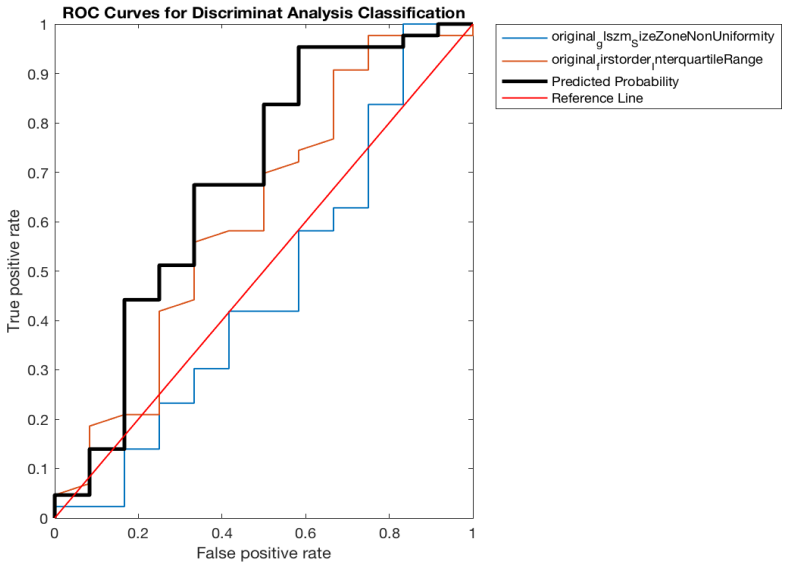

(B)

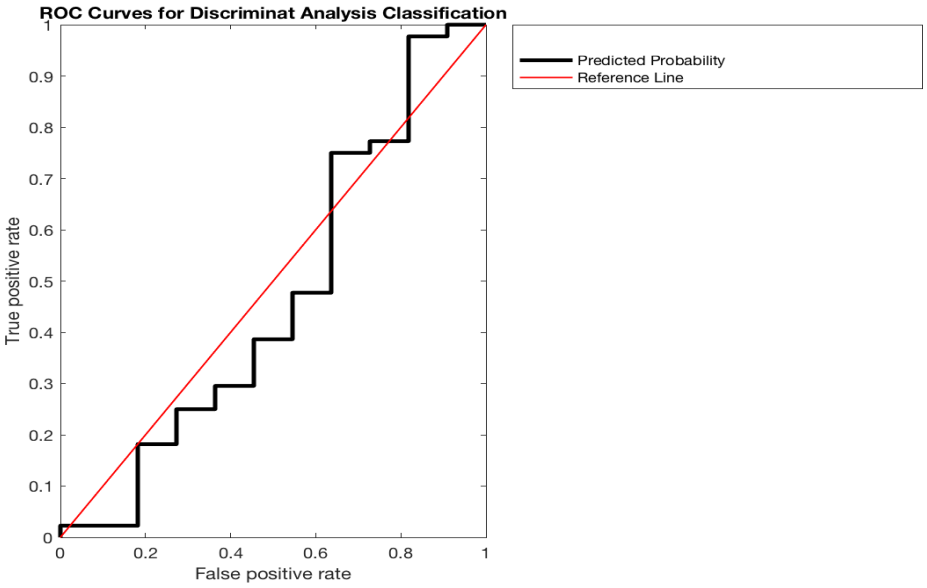

Figure 11 – ROC curve of the most discriminating feature on the arterial **(A)** and portal **(B)** phases for the prediction of Vascular invasion.

(A)

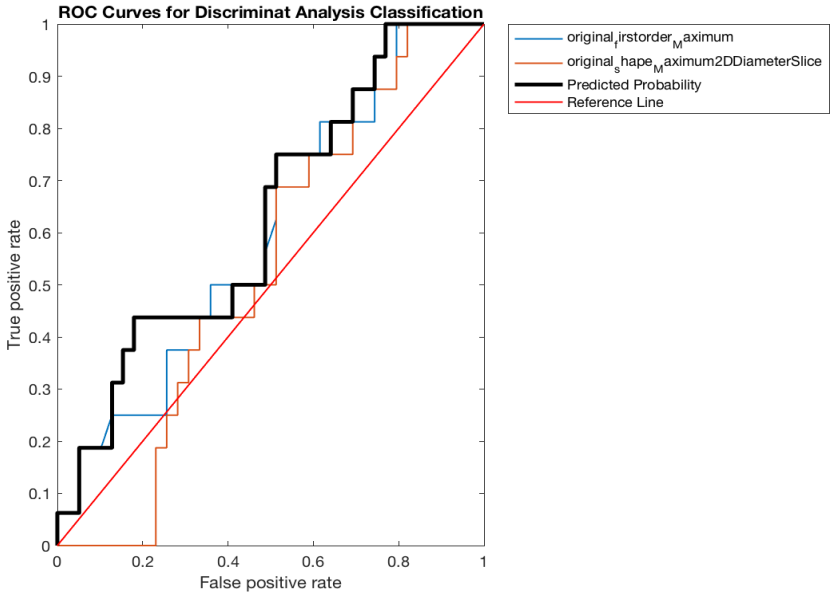

(B)

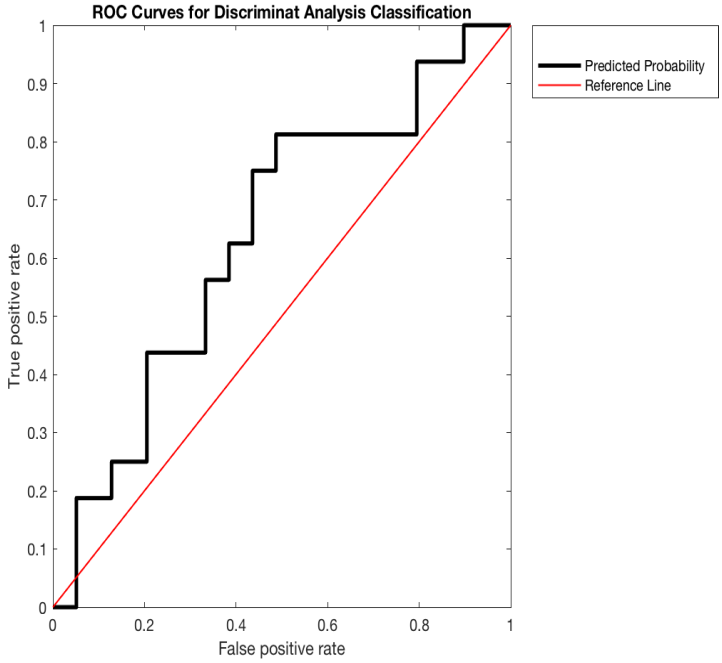

Figure 12 – ROC curve of the most discriminating feature on the arterial **(A)** and portal **(B)** phases for the prediction of Lymph node metastases.

(A)

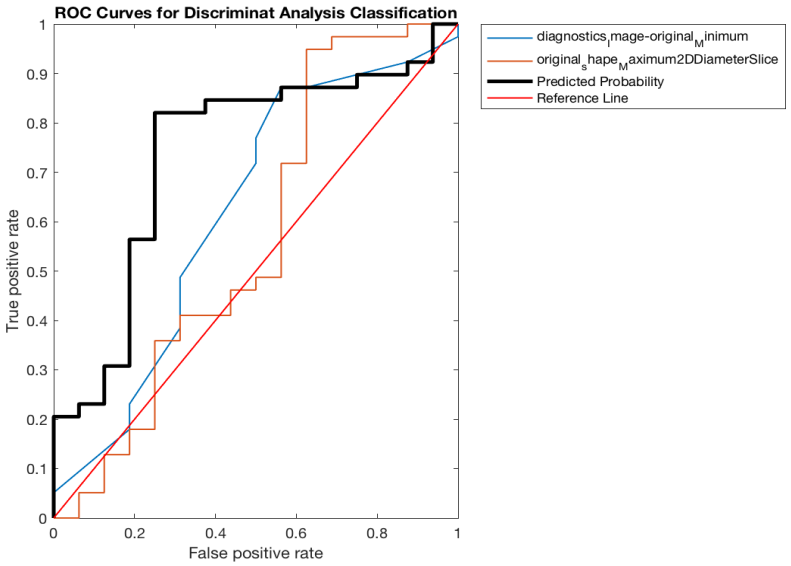

(B)

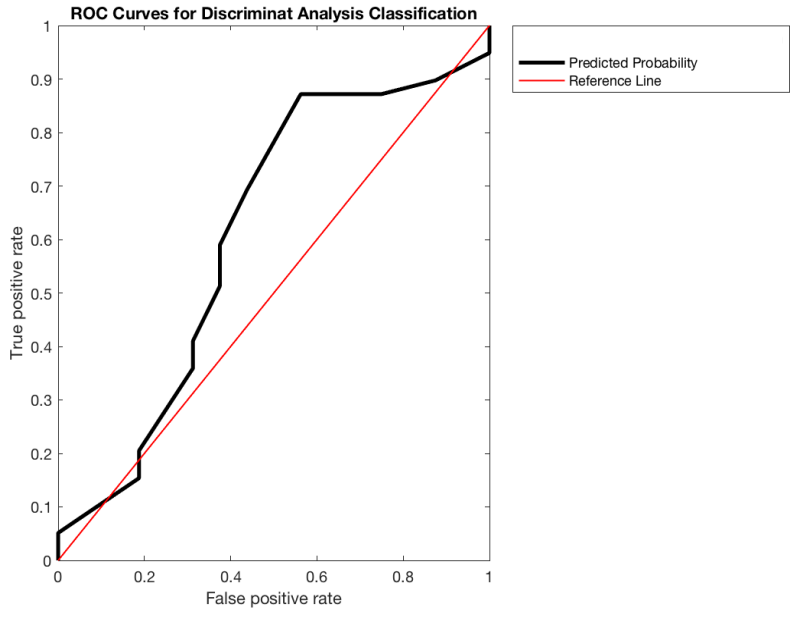

Figure 13 – ROC curve of the most discriminating feature on the arterial **(A)** and portal **(B)** phases for the prediction of Margins.

(A)

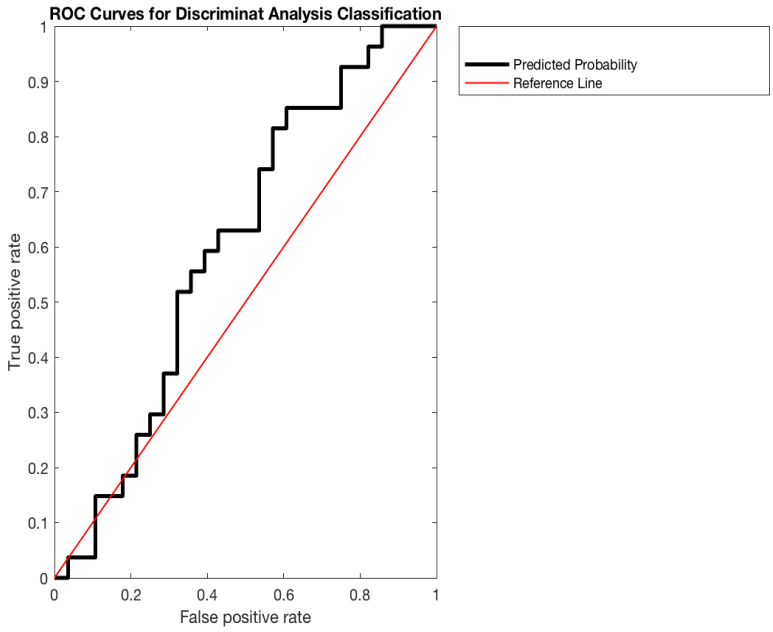

(B)

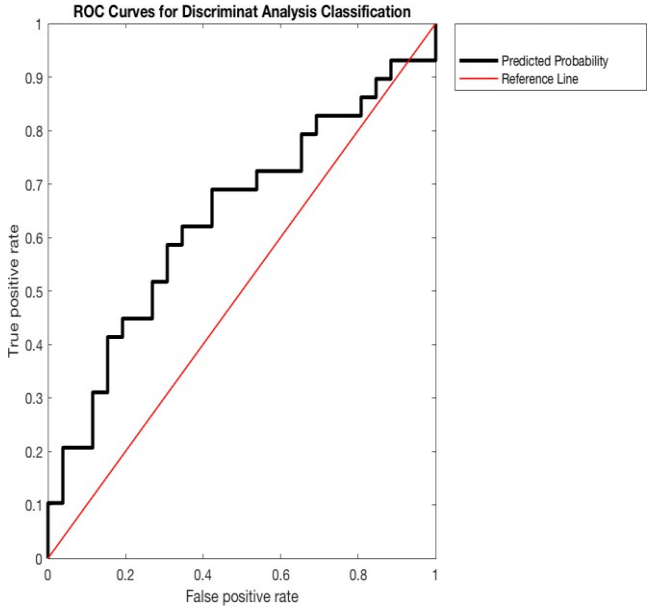

As illustrated in Table 4, the proportion of radiomic features demonstrating reproducibility with ICC > 0.80 was 33% among experienced radiologists and 24% among non-expert radiologists. Across both arterial and portal phases, reliability among all four observers was excellent for aspects such as adherence to the 0 value of 4/5 (80%) of the reference standard (ICC = 0.73-0.75), tumor positioning within the body- tail region (ICC = 0.73-0.74), pathological largest diameter of the tumor (ICC = 0.73-0.78), and absence of biliary stents (ICC = 0.73-0.74).

Moreover, reproducibility of radiomic features displayed an inverse relationship with the aggressiveness of histological parameters, exhibiting poor reliability values in the presence of vascular invasion (ICC = 0.24). Conversely, reliability was directly proportional to tumor size, showcasing excellent reliability values for larger tumors (ICC > 0.80).

Table 4 – Outcomes evaluated using ICC to demonstrate the robustness and reliability of the radiomics analysis across different observers.

Outcome	ICC Arterial phase			ICC Portal phase		
	All 4 observers	Observers 1-3	Observers 2-4	All 4 observers	Observers 1-3	Observers 2-4
Differentiation **0** **1**	0.88 0.63	0.75 0.63	0.75 0.63	0.88 0.74	0.73 0.71	0.73 0.71
Perineural invasion **0** **1**	0.85 0.56	0.74 0.41	0.74 0.41	0.88 0.56	0.74 0.33	0.74 0.33
Vascular invasion **0** **1**	0.86 0.24	0.75 -0.04	0.75 -0.04	0.88 0.29	0.73 0.06	0.73 0.06
Lymph node metastases **0** **1**	0.87 0.63	0.74 0.62	0.74 0.62	0.88 0.67	0.73 0.63	0.73 0.63
Margins **0** **1**	0.63 0.87	0.11 0.77	0.11 0.77	0.72 0.88	0.25 0.79	0.25 0.79
Location **0** **1**	0.87 0.63	0.74 0.62	0.74 0.62	0.88 0.67	0.73 0.62	0.73 0.62
Pathological diameter **0** **1**	0.48 0.85	0.08 0.73	0.08 0.73	0.48 0.88	-0.02 0.78	-0.02 0.78
Stent **0** **1**	0.85 0.63	0.74 0.40	0.74 0.40	0.88 0.74	0.73 0.59	0.73 0.59

2.4 DISCUSSION

Radiomics represents a novel methodology grounded in segmentation and extraction algorithms, facilitating the acquisition of quantitative data from radiological images that are otherwise imperceptible to the naked eye. Our retrospective study, initiated in 2020, stems from a collaborative effort between Paolo Giaccone University Hospital and the "La Maddalena" level III Oncology Department. It juxtaposes and integrates radiological and histological reports of 57 patients diagnosed with pancreatic ductal adenocarcinoma. These patients underwent contrast- enhanced CT scans followed by surgical resection of the lesion and subsequent histopathological analysis.

The study's aim is to validate the efficacy of radiomics in characterizing pancreatic ductal adenocarcinoma by evaluating lesions in both arterial and portal CT phases. Histopathological parameters such as grading, vascular invasion, perineural invasion, margin involvement, and lymph node metastases serve as reference standards. Promising results were achieved, particularly in predicting poorly differentiated lesions, across both arterial and portal phases.

The clinical significance of these findings lies in the ability to non- invasively and accurately identify poorly differentiated pancreatic ductal adenocarcinoma. This facilitates the initiation of chemo-/neoadjuvant radiotherapy prior to surgery, thereby enhancing the patient's survival prospects during adenocarcinoma resection.

Identifying and pre-emptively treating poorly differentiated pancreatic ductal adenocarcinoma represents a scientific advancement aimed at improving prognosis, optimizing clinical timelines, enhancing patient compliance, and mitigating the psychophysical stress associated with potentially unfavorable surgical outcomes.

Our study's outcomes align with recent scientific literature, which underscores the efficacy of machine learning tools in analyzing pancreatic lesion texture and predicting histological grading. Notable studies by Qiu (2019) (54), Kulkarni (2020) (55), and Chang (2020) (56) corroborate our findings, highlighting the potential of radiomics in evaluating histological outcomes.

However, our study is not without limitations. These include its retrospective nature, the limited patient cohort, the absence of MRI data - justified by the infrequent use of MRI in studying these lesions - and the lack of an external validation cohort.

This study is designed to showcase the reliability of CT radiomic features in comparison to histological parameters, which serve as pivotal reference standards in determining the operability of tumor predicting overall patient survival rates. The findings of our research indicate that the robustness of CT radiomic features tends to decrease when confronted with more aggressive histological characteristics, although an exception is noted in the case of larger tumors. This phenomenon can be attributed to the complex and infiltrative nature of aggressive tumors, which poses challenges in accurately delineating lesions on CT scans. The difficulty in segmentation arises due to the intricate boundaries of such tumors, making them less distinguishable on CT images.

On the flip side, when dealing with larger tumors, their increased size might actually aid in achieving clearer delineation of the tumor margins, thereby enhancing the accuracy of segmentation. Concerning the size factor, numerous studies have conducted comparative analyses between the predictive abilities of radiomics and those of the TNM clinical staging system, consistently demonstrating that radiomics outperforms the TNM staging system (57) (58).

Given that radiomic analyses are primarily focused on a specific region of interest, typically the primary tumor, and involve fewer data points beyond the tumor boundaries, it was conjectured that the augmented prognostic value stemmed from extracting more comprehensive information beyond just the tumor size. Moreover, an important consideration in patients with pancreatic cancer is the potential development of biliary strictures necessitating the insertion of metallic stents within the bile duct.

The presence of these biliary stents introduces a notable decrease in robustness, as reported in the literature (59) (60), primarily due to the occurrence of beam-hardening artifacts caused by the metallic composition of the devices. These artifacts detrimentally impact the quality of CT images by distorting pixel intensities and introducing streaking effects, thereby impeding the accurate evaluation of pancreatic lesions. Consequently, the compromised image quality resulting from beam-hardening artifacts poses a significant challenge in precisely characterizing and assessing the extent of pancreatic lesions in patients with biliary stents.

2.5 CONCLUSION

This study presents promising findings regarding the application of radiomics in predicting histological grading and distinguishing poorly differentiated PDACs. The methodology involved extracting data from specific regions of interest identified in contrast-enhanced CT scans conducted during both arterial and portal phases of imaging.

Furthermore, the study brought to light an important observation regarding the reproducibility of radiomic features, particularly in the context of varying histological parameters. It was noted that the reproducibility of these features significantly diminishes when confronted with more aggressive histological characteristics. This phenomenon suggests a prominent role of segmentation uncertainty, particularly evident in advanced PDAC cases. Segmentation uncertainty refers to the difficulty in accurately delineating tumor boundaries due to the complex and infiltrative nature of aggressive tumors, which leads to variability in the extracted radiomic features.

Conversely, the study also revealed that higher reproducibility of radiomic features was observed in cases involving larger tumor dimensions. This finding underscores the significance of tumor volume in influencing segmentation variability and the stability of radiomic characteristics. Larger tumors typically exhibit clearer and more discernible boundaries, facilitating more consistent segmentation and extraction of radiomic features.

In summary, the study highlights the potential of radiomics in predicting histological grading and identifying poorly differentiated PDACs. However, it also emphasizes the challenges associated with segmentation uncertainty, particularly in the context of

aggressive tumor phenotypes, while acknowledging the influence of tumor size on the reproducibility of radiomic features.

3 REFERENCES

1. Siegel RL, Miller KD, Fuchs HE, Jemal A (2021) Cancer Statistics, 2021. CA Cancer J Clin 71:7–33.
2. Mahul B, Amin SBE, Greene FL, Byrd DR, Brookland RK (2017) In: Washington MK, Gershenwald JE, Compton CC, Hess KR, Sullivan DC, Milburn Jessup J, Brierley JD, Gaspar LE, Schilsky RL, Balch CM, Winchester DP, Asare EA, Madera M, Gress DM, Meyer LR (eds) AJCC Cancer Staging Manual, 8th edn, Springer, Cham.
3. Sun H, Ma H, Hong G, Sun H, Wang J (2014) Survival improvement in patients with pancreatic cancer by decade: a period analysis of the SEER database, 1981-2010. Sci Rep 4:6747
4. "Il tumore del Tumore Pancreas - "Il tumore del pancreas." Tumore Pancreas-Codice viola. Available:https://tumorepancreas.codiceviola.org/tumore-del-pancreas/.
5. "Tumore al pancreas." Osservatorio Malattie Rare. Available: https://www.osservatoriomalattierare.it/i-tumori-rari/tumore-al-pancreas/15389-adenocarcinoma-al-pancreas-entro-il-2030-sara-la- seconda-causa-di-morte-tra-i-tumori.
6. "Estimated age-standardized incidence rates (World) in 2022, pancreas, both sexes, all ages." GCO Cancer Today.
   Available: https://gco.iarc.who.int/media/globocan/factsheets/cancers/39-all-cancers-fact-sheet.pdf.
7. Rawla P., Sunkara T., Gaduputi V. Epidemiology of Pancreatic Cancer: Global Trends, Etiology and Risk Factors. World journal of oncology. 2019, p. 10-27.

8. Siegel R. L., Miller K. D., Fuchs H., Jemal A. Cancer statistics, 2021. A Cancer Journal for Clinicians. 2021, p. 7-33.
9. GLOBOCAN estimates of incidence and mortality worldwide for 36 cancers in 185 countries. F. Bray, J. Ferlay, I. Soerjomataran, et al. 2018, Global cancer statistics, p. 394-424.
10. Taunk P., Hecht E., Stolzenberg-Solomon R. Are meat and heme iron intake associated with pancreatic cancer? results from the NIH-AARPdiet and health cohort. Int J Cancer. 138, 2016, p. 2172-2189.
11. Larsson S.C., Wolk A. Red and processed meat consumption and risk of pancreatic cancer: meta-analysis of prospective studies. Br J Cancer. 2012, p. 603-607.
12. Alsamarrai A., Das S.L.M., Windsor J.A. et al. Factors that affect risk for pancreatic disease in the general population: a systematic review and meta-analysis of prospective cohort studies. Clin Gastroenterol Hepatol. 12, 2014, p. 1635-1644.
13. Wu Q.-J., Wu L.-Q et al. Consumption of fruit and vegetables reduces risk of pancreatic cancer: evidence from epidemiological studies. Eur J Cancer Prev. 25, 2016, p. 196-205.
14. Natalia Khalaf, Hashem B. El-Serag, Hannah R. Abrams, Aaron P. Thrift. Burden of Pancreatic Cancer: From Epidemiology to Practice. Clinical Gastroenterology and Hepatology. 2021, Vol. 19,5.
15. Quanxiao Li, Meng Jin, Yahui Liu, Limin Jin. Gut Microbiota: its potential roles in pancreatic cancer. Frontiers in cellular and infection microbiology. 7 Oct 2020, Vol. 10.
16. Hu, H.-F., Ye, Z., Qin, Y., Xu, X.-W., Yu, X.-J., Zhuo, Q.-F., & Ji, S.-R. Mutations in key driver genes of pancreatic cancer: molecularly targeted therapies and other clinical implications. Acta Pharmacologica Sinica. 2021.

17. Daniel S. Longnecker, Richard M. Goldberg. Pathology of exocrine pancreatic neoplasm. UpToDate. [Online] 21 Gennaio 2021. https://www.uptodate.com/contents/pathology-of-exocrine-pancreatic-neoplasms?search=neoplasm%20pancreas%20hystopathology&source =search_result&selectedTitle=2~150&usage_type=default&display_ra nk=2 #H6.

18 Khoschy Schawkat, Maria A. Manning, Jonathan N. Glickman, and Koenraad J. Mortele. Pancreatic Ductal Adenocarcinoma and Its Variants: Pearls and Perils. RadioGraphics. 2020, Vol. 40:5, p. 1219-1239.

19 D'Haese, J.G., Werner, J. Resektabilität des Pankreaskarzinoms. Radiologe 56, 318–324 (2016).

20 D. Bell. Cross-sectional Imaging. Radiopaedia.org. [Online] 1 Oct 2017. https://radiopaedia.org/articles/cross-sectional- imaging-1. rID: 55943.

21 Kulkarni, N. M., Hough, D. M., Tolat, P. P., Soloff, E. V., & Kambadakone, A. R. Pancreatic adenocarcinoma: cross-sectional imaging techniques. Abdominal radiology (New York). 2018, Vol. 43(2).

22 Al-Hawary, M. M., Francis, I. R., Chari, S. T., Fishman, E. K., Hough, D. M., Lu, D. S., Macari, M., Megibow, A. J., Miller, F. H., Mortele, K. J., Merchant, N. B., Minter, R. M., Tamm, E. P., Sahani, D.V., & Simeone, D.M. Pancreatic ductal adenocarcinoma radiology reporting template: consensus statement of the society of abdominal radiology and the American pancreatic association. Gastroenterology. 146, 2014, Vol. 1, p. 291-304.

23 Almeida, R. R., Lo, G. C., Patino, M., Bizzo, B., Canellas, R., & Sahani, D. V. Advances in Pancreatic CT Imaging. AJR. American journal of roentgenology. 2018, Vol. 211, p. 52-66.

24 Chu LC, Goggins MG, Fishman EK. Diagnosis and detection of pancreatic cancer. The cancer journal Sudbury, Mass. 2017, Vol. 23, 6, p. 333-342.

25 Marion-Audibert A.M., Vullierme M.P., Ronot M., Mabrut J.Y., Sauvanet A., Zins M., Cuilleron M., Sa-Cunha A., Lévy F., Rode A. Routine MRI with DWI Sequences to Detect Liver Metastases in Patients With Potentially Resectable Pancreatic Ductal Carcinoma and Normal Liver CT: A Prospective Multicenter Study. . AJR Am. J. Roentgenol. 2018, 211:217– 225.

26 Klauss M, Schobinger M, Wolf I, Werner J, Meinzer HP, Kauczor HU, Grenacher L. Value of three-dimensional reconstructions in pancreatic carcinoma using multidetector CT: initial results. World J Gastroenterology. 2009.

27 Silvestris, N., Brunetti, O., Bittoni, A., Cataldo, I., Corsi, D., Crippa, S., D'Onofrio, M., Fiore, M., Giommoni, E., Milella, M., Pezzilli, R., Vasile, E., & Reni, M. Clinical Practice Guidelines for Diagnosis, Treatment and Follow- Up of Exocrine Pancreatic Ductal Adenocarcinoma: Evidence Evaluation and Recommendations by the Italian Association of Medical Oncology (AIOM). Cancers. 12(6), 1681, (2020).

28 Frank G Gress, Douglas A Howell, Kristen M Robson. Endoscopic ultrasound in the staging of exocrine pancreatic cancer.2020.

29 Moore, A., & Donahue, T. (2019). Pancreatic Cancer. JAMA,322(14), 1426.

30 C. F. del Castillo, R. E. Jimenez, S. W. Ashley, K. K. Tanabe, W. Chen. Overview of surgery in the treatment of exocrine pancreatic cancer and prognosis. s.l.: UpToDate, May 04 2020.

31 Janssen, Q.P. O'Reilly E.M., van Eijck C., Groot Koerkamp B. Neoadjuvan Treatmen in patients with resectable and borderlineresectable pancreatic cancer. Frontiers in oncology. Jan 31 2020, Vol. 10, 41, p. 10, 41.

32 M., Singh R. R. & O'Reilly E. New Treatment strategies for metastatic pancreatic ductal adenocarcinoma. Drugs. 80, 2020, Vol. 7, p. 647-669.

33 Daniel S Longnecker, Richard M Goldberg, Diane MF Savarese. Pathology of exocrine pancreatic neoplasms. s.l.: In: UpToDate, Post TW (Ed), UpToDate, Waltham, MA., Jan 21, 2021.

34 Marius E. Mayerhoefer, Andrzej Materka, Georg Langs, Ida Häggström, Piotr Szczypiński , Peter Gibbs e Gary Cook. Introduction to radiomics. Journal of nuclear medicine. 61, April 2020, Vol. 4, p. 488-495.

35 Hatt, M., Le Rest, C. C., Tixier, F., Badic, B., Schick, U., & Visvikis, D. Radiomics: data are also images. Journal of nuclear medicine: official publication, Society of nuclear medicine. 60, 2019, Vol. (Suppl 2), p. 38S- 44S.

36 Ming He, Huadan Xue, Zhengyu Jin. Radiomics in pancreatic ductal adenocarcinoma: a state of art review. Journal of Pancreatology (2020) 3:4.

37 Deep learning. Intelligenza Artificiale. [Online] https://www.intelligenzaartificiale.it/deep- learning/#Cos8217e_il_deep_learning.

38 Van Timmeren, J., Cester, D., Tanadini-Lang, S. et al. Radiomics in medical imaging: "how to" guide and critical reflection. Insight imaging. 11, 2020, Vol. 91.

39 Abunahel, BM, Pontre, B., Kumar, H. et al. Pancreas image mining: a systematic review of radiomics. Eur Radiol. 2021, 31, p. 3447–3467.

40 L. C. Chu, S. Park, S. Kawamoto et al. Utility of CT Radiomics Features in Differentiation of pancreatic ductal adenocarcinoma from normal pancreatic tissue. Gastrointestinal imaging. 2019, Vol. 213, 2, p. 349-357.

41 Y. Zhang, C. Cheng, Z. Liu et al. Radiomics analysis for the differentiation of autoimmune pancreatitis and p ancreatic ductal adenocarcinoma in 18F-FDG PET/CT. Med Phys. 46, 2019, Vol. 10, p. 4520- 4530.

42 He M, Liu Z, Lin Y, et al. Differentiation of atypical non- functional pancreatic neuroendocrine tumor and pancreatic ductal adenocarcinoma using CT based radiomics. European Journal of Radiology. 117, 2019, p. 102-111.

43 Huang Z, Li M, He D, Wei Y, Yu H, Wang Y, Yuan F, Song B. Two- dimensional Texture Analysis Based on CT Images to Differentiate Pancreatic Lymphoma and Pancreatic Adenocarcinoma: A Preliminary Study. Acad Radiol. 26, 2019, Vol. 8, p. e189-e195.

44 Park S, Chu LC, Hruban RH, Vogelstein B, Kinzler KW, Yuille AL, Fouladi DF, Shayesteh S, Ghandili S, Wolfgang CL, Burkhart R, He J, Fishman EK, Kawamoto S. Differentiating autoimmune pancreatitis from pancreatic ductal adenocarcinoma with CT radiomics features. Diagn Interv Imaging. 101, 2020, Vol. 9, p. 555-564.

45 Shi, H., Wei, Y., Cheng, S., Lu, Z., Zhang, K., Jiang, K., & Xu, Q. Survival prediction after upfront surgery in patients with pancreatic ductal adenocarcinoma: Radiomic, clinic-pathologic and body composition analysis. Pancreatology: official journal of the International Association of Pancreatology (IAP). 21, 2021, 4, p. 731-737.

46 Van Griethuysen JJM, Fedorov A, Parmar C, et al. Computational radiomics system to decode the radiographic phenotype. Cancer 12 Technology in Cancer Research & Treatment Res. 2017;77(21): e104-e1e7. doi: 10.1158/0008-5472.CAN-17- 0339. PubMed PMID: 29092951; PubMed Central PMCID: PMCPMC5672828.

47 Patriarca, Silvia. Elementi di stadiazione dei tumori e sistema TNM. Registri Tumori. [Online] 10 maggio 2010.

48 Jennifer F. Tseng, Eric P. Tamm, Jeffrey E. Lee, Peter W.T. Pisters, Douglas B. Evans. Venous resection in pancreatic cancer surgery. Best Practice & Research Clinical Gastroenterology. 2006, Vol. 20, 2, p. 349- 364.

49 Van Roessel, S., Kasumova, G.G., Tabatabaie, O. et al. Pathological Margin Clearance and Survival After Pancreaticoduodenectomy in a US and European Pancreatic Center. Ann Surg Oncol 25, 1760–1767 (2018).

50 Chang, D. K., Johns, A. L., Merrett, N. D., Gill, A. J., Colvin, E. K., Scarlett, C. J., Nguyen, N. Q., Leong, R. W., Cosman, P. H., Kelly, M. I., Sutherland, R. L., Henshall, S. M., Kench, J. G., & Biankin, A. V. Margin clearance and outcome in resected pancreatic cancer. Journal of clinical oncology: official journal of the American Society of Clinical Oncology, 27, 2009, Vol. 17, p. 2855-2862.

51 Hermanek, P., & Wittekind, C. The pathologist and the residual tumor (R) classification. Pathology, research and practice. 1994, Vol. 190, 2, p. 115-123.

52 Patel, B.N., Olcott, E. & Jeffrey, R.B. Extrapancreatic perineural invasion in pancreatic adenocarcinoma. Abdominal Radiology. 2018, 43, p. 323-331.

53 Pawlik, T. M., Gleisner, A. L., Cameron, J. L., Winter, J. M., Assumpcao, L., Lillemoe, K. D., Wolfgang, C., Hruban, R. H., Schulick, R. D., Yeo, C. J., & Choti, M. A. Prognostic relevance of lymph node ratio following pancreaticoduodenectomy for pancreatic cancer. Surgery. 2007, Vol. 141, 5, p. 610-618.

54 Qiu, W., Duan, N., Chen, X., Ren, S., Zhang, Y., Wang, Z., & Chen, R. Pancreatic Ductal Adenocarcinoma: Machine Learning-Based Quantitative Computed Tomography Texture Analysis For Prediction Of Histopathological Grade. Cancer management and research. 11, 2019, p. 9253-9264.

55 Kulkarni, A., Carrion-Martinez, I., Jiang, N. N., Puttagunta, S., Ruo, L., Meyers, B. M., Aziz, T., & van der Pol, C. B. Hypovascular pancreas head adenocarcinoma: CT texture analysis for assessment of resection margin status and high-risk features. European radiology.30(5), 2020, p. 2853– 2860.

56 Chang, N., Cui, L., Luo, Y., Chang, Z., Yu, B., & Liu, Z. Development and multicenter validation of a CT-based radiomics signature for discriminating histological grades of pancreatic ductal adenocarcinoma. Quantitative imaging in medicine and surgery. 10 (3), 2020, p. 692-702.

57 Healy GM, Salinas-Miranda E, Jain R et al (2021) Pre-operative radiomics model for prognostication in resectable pancreatic adenocarcinoma with external validation. Eur Radiol 32:2492–2505.

58 Xie T, Wang X, Li M, Tong T, Yu X, Zhou Z (2020) Pancreatic ductal adenocarcinoma: a radiomics nomogram outperforms clinical model and TNM staging for survival estimation after curative resection. Eur Radiol 30:2513–2524.

59 Garima Suman, Anurima Patra, Sovanlal Mukherjee, Panagiotis Korffiatis and Ajit H. Goenka. Radiomics for Detection of Pancreas Adenocarcinoma on CT Scans: Impact of Biliary Stents. Radiology: Imaging Cancer Volume 4: Number 1—2022.

60 Lambin P, Leijenaar RTH, Deist TM, et al. Radiomics: the bridge between medical imaging and personalized medicine. *Nat Rev Clin Oncol* 2017;14(12):749–762.